Vibrational Heating Efficiency of LiH Molecules in Collision with He Atoms†

E. Bodo, S. Kumar,‡ and F. A. Gianturco*

Department of Chemistry, The University of Rome, Cittá Universitaria, 00185 Rome, Italy

A. Famulari, M. Raimondi, and M. Sironi

Department of Physical Chemistry and Electrochemistry, CNR Center CSRSRC, University of Milan, via Golgi 19, 22133, Milan, Italy

Received: March 11, 1998; In Final Form: June 12, 1998

The full Born−Oppenheimer (BO) potential energy surface that describes the interaction between a vibrating and rotating LiH molecule and an He atom, obtained from ab initio VB calculations described before (*Chem. Phys.* **1997**, *215*, 287), is employed here to evaluate the corresponding partial integral cross sections over a range of energies of astrophysical relevance. The process examined involves rotovibrational heating of the initially "cold" target molecule in a single-collision situation, and it provides specific indications on the process efficiency for modeling global kinetics of primordial clouds. The details of the dynamical coupling produced and some specific features of the potential energy surface are analyzed in relation to the behavior of the inelastic cross sections. The average energy transfer values and the relaxation rates are obtained from quantum dynamics and found to be unexpectedly large for such a weakly interacting system.

1. Introduction

The search for the possible presence of LiH and LiH^+ molecular species in the interstellar medium has been intensified in recent years because of the role that such molecules are expected to play in the early universe chemistry (EUC).

As the universe expanded, in fact, atoms and molecules were formed from the free nuclei and electrons, as photoionization and photodissociation gradually became ineffective due to the cooling of the radiation temperature. The matter temperature, T_m, and the radiation temperature, T_r, remained largely the same until a red shift (z) of about 1300 was reached, marking the beginning of the recombination era, after which the Compton scattering was no longer able to overcome the cooling by the expansion and the values of T_m became lower than those of T_r.[1] The primordial matter therefore continued to cool until collapse was initiated in the protogalactic clouds.

Chemistry was expected to begin with the appearance of the first neutral molecule H_2 soon after the production of neutral atomic hydrogen through the radiative recombination of protons and electrons. The specific chemistry involving lithium, on the other hand, was initiated by the recombination of Li which occurred, at z values around 450, through radiative recombination,

$$Li^+ + e \rightarrow Li + h\nu \quad (1)$$

or by mutual neutralization,

$$Li^+ + H^- \rightarrow Li + H \quad (2)$$

With the production of neutral lithium, the LiH molecule would then be formed by radiative association,[2]

$$Li + H \rightarrow LiH + h\nu \quad (3)$$

and by associative detachment,

$$Li + H^- \rightarrow LiH + e^- \quad (4)$$

The above reactions are likely to initially form the title molecule in rotovibrationally excited states, which could then radiate through spontaneous or stimulated emission processes.

In the absence of heavier elements, the radiative cooling at temperatures of less than 8000 K is controlled by the presence of a small fraction of the gas that has become molecular, and it is the molecular cooling that then allows the primordial clouds to collapse.[3] The details of the cooling mechanisms are therefore important for the determination of both the large-scale structure, represented by globular cluster and galaxy masses, and the small-scale structure, represented by the initial mass function. At the onset of the collapse the relative molecular abundances, as evolved from the postrecombination period, provide a constraint for the cooling processes and therefore influence the initial galactic and stellar evolution of the universe.[4] It has been suggested, therefore, that primordial molecules with large permanent dipole moments might become detectable by their radiative imprint in the cosmic background radiation (CBR) arising from the resonant enhancement of the Thompson scattering cross sections which can occur at the transition frequencies of such molecules.[5]

More specifically, the effects of the presence of LiH in the early universe have been recently explored experimentally,[6] although the final answer is still not unequivocally clear. It is therefore important to be able to analyze more in detail the actual efficiency of various possible processes that could lead to the formation of rotationally and/or vibrationally "hot" LiH

† This work is dedicated to our friend and colleague Raphy D. Levine, on the occasion of his 60th birthday and with our most sincere wishes to continue for many more years his outstanding contributions to the field of molecular dynamics processes.

‡ Present address: Tata Institute of Fundamental Research, Hami Bhabha Rd., Mumbai, 400005, India.

10.1021/jp981462q CCC: $15.00
Published on Web 09/09/1998

molecules by collision with the most common partners such as He, H, and H^+.

It should also be made clear that in order to be able to provide a more realistic global modeling of the EUC discussed before, many more possible mechanisms, besides the few mentioned above, need to be included and need to be known both as kinetic rates and as elementary processes.[7] On the other hand, given how little we know at the quantitative level about the energy exchange efficiency between the species of largest abundance and the molecular candidates that appear among the most likely sources of CBR anisotropy, it is indeed important to start to put together a more realistic picture and to analyze from first principles the heating efficiency and the relaxation rates of LiH molecules in the presence of other atomic and molecular partners.

We have already discussed the excitation mechanisms that can yield rotationally "hot" lithium hydride molecules after collision with He atoms.[8] In the present work we wish to extend this analysis to the case where the vibrational levels of that molecule are also being excited by low-energy collisions.

One should also keep in mind, however, that given the relative lower abundance of He with respect to H in the interstellar clouds, the latter process is likely to play an even more important role in modeling the global kinetics. It is still relevant, on the other hand, to be able to rely on more realistic rate constants when dealing with the former collision partner.

In the following section we describe the general features of the ab initio potential energy surface (PES) that has been used[9] to obtain the coupling between the He motion and the LiH rotovibrational motion, while section 3 reports the quantum dynamics involved in the collisional excitation modeling. Section 4 describes then the cross section behavior and the effects on the decoupling approximations. Section 5 finally reports the excitation and relaxation rates over a broad range of temperatures, together with the average energy transfer indices. Our present conclusions are summarized in section 6.

2. The Vibrational Interaction

As discussed in our previous work,[9] the fully ab initio potential energy surface was computed as a function of the usual three Jacobi coordinates, R, r, and γ, where the atom−diatom distance R is taken from the target center-of-mass and the $\gamma = 0°$ orientation corresponds to the Li−H−He configuration. The calculations followed the spin-coupled valence bond (SCVB) configuration interaction (CI) treatment already discussed earlier in great detail,[10] and we will therefore not repeat here its derivation. Suffice it to say that the spin-coupled (SC) wave function for a van der Waals (vdW) complex is based on the antisymmetrized product of a single string of distinct, singly occupied nonorthogonal orbitals and a fully optimized spin eigenfunction. The further configurations which are included in the subsequent nonorthogonal CI calculation are then generated by excitations from the occupied orbitals into virtual orbitals associated with the same fragment. To avoid the basis set superposition error (BSSE) which is frequently altering the features of the interaction in weakly interacting partners,[10] each of the SC occupied and virtual orbitals is expanded using only the basis functions from the relevant fragment. With a judiciously chosen basis set, one can therefore show that the resulting BSSE-free potential energy surfaces can indeed provide very accurate data. At each geometry, we determined first the six SC orbitals pertaining to the ground-state configuration and then optimized a set of four virtual orbitals, considering the simultaneous single excitations of LiH valence electrons and of He electrons. This optimized set of six occupied and four virtual orbitals was then used within a fully variational SCVB calculation. As in our previous study,[11] we found here that this very compact expansion, consisting of just 25 VB structures, produced overall accuracy that was comparable to that previously achieved in a more standard SCVB calculation based on 15 virtual orbitals per active electron and on 2005 VB structures.[11] Even the very small minimum of the present PES of about 0.01 mhartrees at $\gamma = 0°$ and $R = 11\ a_0$ (with r at its equilibrium value of 3.0139 a_o) was well reproduced by the optimized, compact set of structures employed in the present work.[9]

Using the above strategy, we computed 144 values of the orientational and of the distance coordinates (12 values of γ and 12 values of R) for each of the chosen values of r. The latter five different values were selected by first constructing the LiH potential curve as a Morse function with the experimental parameters. We then set the r_1 and r_5 values to be the vibrational turning points for the $\nu = 4$ bound state of the isolated diatomic target (i.e., 2.293 64 and 4.304 73 bohr, respectively). As the r_3 value we chose the ground electronic state equilibrium bond length mentioned before. Finally, the two remaining values were chosen as $r_2 = (r_1+r_3)/2$ and $r_4 = (r_3+r_5)/2$, i.e., 2.653 87 and 3.659 32 bohr, respectively.

The overall representation of the full surface, now given by a total of $144 \times 5 = 720$ points, has also been given in detail before[9] and will therefore only be briefly outlined here.

We thus followed the strategy adopted in earlier work[12] so that the ab initio interaction energies were used to construct an analytic representation $V(R,\gamma)$ expanded in the familiar Legendre polynomials

$$V(R,\gamma) = \sum_{\lambda=0}^{\lambda_{max}} V_\lambda(R)\, P_\lambda(\cos\gamma) \tag{5}$$

with the radial coefficients $V_\lambda(R)$ being further expanded in Laguerre polynomials

$$V_\lambda(R) = \sum_{k=0}^{k_{max}} A_{k\lambda} L_k[\alpha_\lambda(R-a)] \exp\left(-\frac{1}{2}\alpha_\lambda(R-a)\right) \tag{6}$$

The parameters α_λ were determined by minimizing the square of the deviations between the ab initio and fitted surfaces, as described before.[9] We used $a = 3.7330\ 94$ bohr for the three smallest values of r and $a = 5.0768\ 45$ bohr for the two larger values of r.

It follows from the orthogonality properties of the Laguerre polynomials that

$$A_{k\lambda} = \alpha_\lambda \int_a^\infty V_\lambda(R)\, L_k[\alpha_\lambda(R-a)] \exp\left(-\frac{1}{2}\alpha_\lambda(R-a)\right) \mathrm{d}R \tag{7}$$

and from the orthogonality properties of Legendre polynomials that

$$V_\lambda(R) = \frac{1}{2}(2\lambda+1)\int_0^\pi V(R,\gamma)\, P_\lambda(\cos\gamma) \sin\gamma\, \mathrm{d}\gamma \tag{8}$$

Combining eqs 7 and 8, we obtain

$$A_{k\lambda} = \frac{1}{2}(2\lambda+1)\alpha_\lambda \int_0^\infty \int_0^\pi \left\{ V(R,\gamma)\, P_\lambda(\cos\gamma) \times L_\lambda[\alpha_\lambda(R-a)] \exp\left(-\frac{1}{2}\alpha_\lambda(R-a)\right) \sin\gamma \right\} \mathrm{d}\gamma\, \mathrm{d}R \tag{9}$$

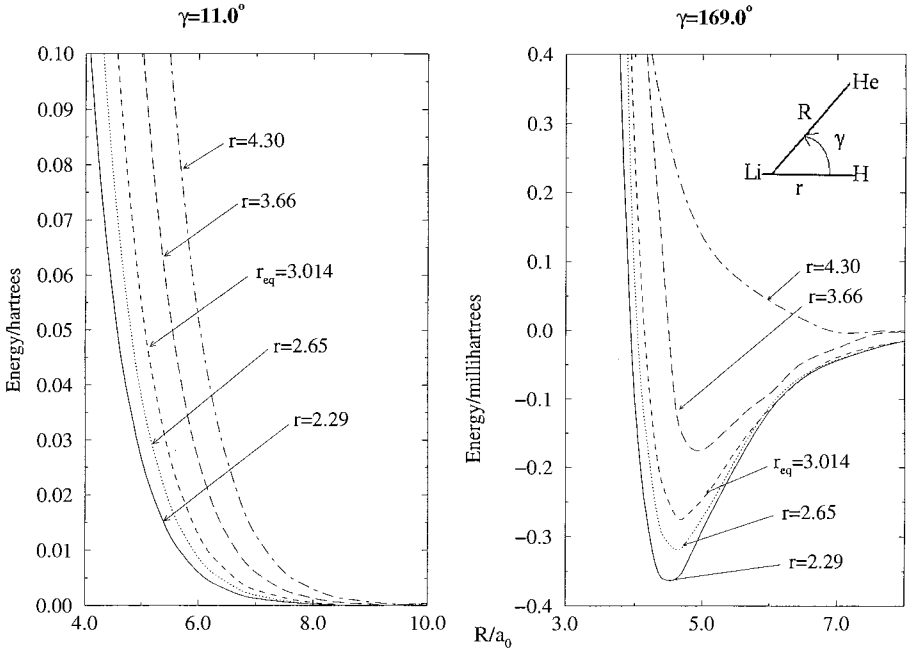

Figure 1. Computed examples of the full potential energy surface at two specific orientations (left and right) and for different values of the target vibrational coordinate. Potential values and distances in atomic units.

The $A_{k\lambda}$ coefficients can easily be evaluated[9] from this last expression using numerical quadrature (Gauss−Laguerre for R and Gauss−Legendre for γ). All the various coefficients have been tabulated and were already given in our previous work.[9]

Just as an example of the behavior of the present surface as a function of the vibrational coordinate, we show in Figure 1 the repulsive region of the interaction (left) and the region of the attractive well (right) for orientation values of $\gamma = 11°$ and $\gamma = 169°$. The various curves refer to different values of the diatomic coordinate. One clearly sees there the following behavior: (i) the stretching of the molecular bond gives rise to a more repulsive interaction as the stretching increases, while the opposite is true when the bond is compressed below its equilibrium value; (ii) such changes are even more dramatically shown by the attractive region, where the shallow well disappears when the molecular bond increases. On the other hand, the attractive potential becomes even more so (with deeper well values) as the bond is compressed.

For the dynamical treatment discussed in the next section, we will make use of the following representation of the potential:

$$V_{ij}(R,\gamma) = \int_{-1}^{1} \chi_i^*(r)\, V(R,\gamma,r)\, \chi_j(r) r^2\, \mathrm{d}r \qquad (10)$$

where χ's are the numerically obtained bound vibrational states of the isolated target in its ground electronic state. Thus, the above quantities (for $i = j$) represent the adiabatically averaged interaction potentials which describe beyond the simpler rigid rotor (RR) approximation the atom−molecule interaction, while the off-diagonal elements are a direct measure of the coupling strength between the molecular vibrations and the perturbation induced by the impinging He atom.

As it is to be expected, and as we have shown already elsewhere,[12] such averaging essentially reproduces the RR interaction for the $v = 0$ and $v \pm 1$ diagonal elements, while the coupling terms turn out to be strongly anisotropic, rather short-range in their R-dependence, and rapidly become negligible as Δv increases from 1 to 2 (i.e., the V_{02} potential coupling is much weaker than the V_{01} term). Thus, one finds from the analysis of the vibrational interaction that the coupling induced by the present potential appears to be strongly dependent on orientation, active only over a limited range of R values and coupling mostly neighboring levels of the target. All the above features will be further analyzed by using the quantum dynamics presented below.

3. The Quantum Dynamics

There have been several coupling schemes for the angular momenta relevant to the dynamics descriptions that have been suggested in the literature[14] over the years. Basically, one tries to decouple some of the molecular degrees of freedom depending upon their relative time scale with respect to the collision interaction times. To solve the vibrational−rotational problem, for example, one generally decouples the rotational motion from the vibrational and translational ones whenever the former remains adiabatic or nearly adiabatic with respect to the other two relative motions. A history of various quantum sudden approximations has been very clearly reviewed by Parker and Pack[15] and, more recently, in ref 16. Strictly speaking, for such a decoupling procedure to work, the interaction time must be short when compared to the rotational period. Such decouplings and their possible failures because of strong dynamical mixing between rotational and vibrational excitation channels in the case of ion−molecule interactions have been extensively discussed by our group.[17,18] It was shown there that one needs a certain amount of caution in applying the infinite order sudden (IOS) treatment, particularly with fast rotors like LiH. As noted in our earlier work,[18] however, the VCC-RIOS (vibrational close coupling rotational IOS) approximation works fairly well for strongly interacting systems like the H^+-H_2 at collision energies $E \geq 3.7$ eV, and therefore we should expect it to be even more realistic for the present neutral system, where short-range interaction and vibrational coupling acting largely in the repulsive region (and at low l values) are present.

The VCC-RIOS scheme has been discussed and documented many times in the literature (e.g., see refs 15, 16 and further references quoted therein). We therefore summarize only the relevant equations.

Starting with the diabatic expansion representation for the total wave function, we can describe the latter with an orthonormal basis of the asymptotic states of the molecular target,

$$\psi_k(R,r,\gamma|k^2) = \sum_{j,v,l} u_k^l(R|k^2)\, Y_{jmj}(\hat{r})\, Y_{lml}(\hat{R})\, \chi_v^{\mathrm{LiH}}(r) \quad (11)$$

where the coefficients depend on the wave vector k^2, the orientations $\hat{r}$ and $\hat{R}$ are referred to as a body-fixed (BF) system with $\cos^{-1}(\gamma) = \hat{r}\cdot\hat{R}$, and the χ_v are the vibrational wave functions of LiH. If we apply the so-called sudden limit, that is, we freeze the relative projectile-to-target orientation during the collision, we have

$$\psi_k^{\vec{j}\bar{l}v}(R,r,\gamma|k^2) = \sum g_{\vec{j}\bar{l}v}(R,\gamma|k^2)\, \chi_v^{\vec{j}}(r)\frac{1}{R} \quad (12)$$

Since the target rotational spacings play no role during the dynamics, the total wave function is thus additionally labeled by the fixed values of the rotational $\vec{j}$ and translational $\bar{l}$ angular momenta (see below). v is now the initial vibrational state of LiH, and k_j^2 is the wave vector selected within the infinite order sudden (IOS) approximations[15] where the centrifugal sudden (CS) simplification has also been applied. For each of the orientation-dependent radial coefficients, g's, and at each collision energy, one now obtains the familiar coupled equations for the vibrational-to-translational (CT) exact energy-transfer dynamics by writing $k_j^2 = k_{\vec{j}v'}^2 = (k_j^2 - 2\mu E_{v'})$.

$$\left\{\frac{\mathrm{d}^2}{\mathrm{d}R^2} - \frac{\bar{l}(l+1)}{R^2} + k_{\vec{j}v'}^2\right\} g_{v'}^{\vec{j}\bar{l}v'}(R|\gamma) = 2\mu\sum_{v'}^{v_{\max}} V_{v'v''}^{\vec{j}}(R|\gamma)\, g_{v'}^{\vec{j}\bar{l}v''}(R|\gamma) \quad (13)$$

Applying the usual boundary conditions to the radial coefficients of eq 12,

$$g_{v'}^{\vec{j}\bar{l}v}(R,\gamma|k^2) \approx \frac{1}{(k_{\vec{j}v'})^{1/2}}\left\{\delta_{vv'}\exp\left[-\mathrm{i}\left(k_{\vec{j}v}R - \bar{l}\frac{\pi}{2}\right)\right] - S_{vv'}^{\vec{j}\bar{l}}(\gamma)\times \exp\left[-\mathrm{i}\left(k_{\vec{j}v}R - \bar{l}\frac{\pi}{2}\right)\right]\right\} \quad (14)$$

$$T_{vv'}^{j'l'}(\gamma) = \delta_{vv'} - S_{vv'}^{j'l'}(\gamma) \quad (15)$$

which, in turn, yields an orientation-dependent cross section for the ($v' \leftarrow v$) process, already summed over all rotational excitations and averaged over all possible rotational degeneracies.

$$\sigma^{\vec{j}}(v' \leftarrow \vec{j}\,v;\, \gamma|k_{\vec{j}}^2) = \frac{\pi}{k_{jv}^2}\sum_{\bar{l}}(2\bar{l}+1)|T_{vv'}^{\vec{j}\bar{l}}(\gamma|k_{\vec{j}}^2)|^2 \quad (16)$$

where $\bar{l}$ is now a simple index over the usual partial wave sum. One finally obtains the real physical observables, that is, the state-to-state cross sections for the particular process, by a quadrature over BF orientations of γ-dependent quantities:[16]

$$\frac{\mathrm{d}\sigma^{\vec{j}}}{\mathrm{d}\Omega}(v' \leftarrow \vec{j}\,v) = \frac{1}{2}\int_{-1}^{1} I^{\vec{j}}(v' \leftarrow v,\, \gamma|\Omega)\, \mathrm{d}(\cos\gamma) \quad (17)$$

$$\sigma^{\vec{j}}(v' \leftarrow \vec{j}\,v|k_{\vec{j}}^2) = \frac{1}{2}\int_{-1}^{1}\sigma^{\vec{j}}(v' \leftarrow v,\, \gamma|k_{\vec{j}}^2)\, \mathrm{d}(\cos\gamma) \quad (18)$$

The vibrational wave functions χ_v's and the corresponding bound state eigenvalues E_v's were determined by the numerical solution of the radial Schrödinger equation as discussed in the previous section, where the actual coupling matrix elements of eq 12 were also briefly discussed.

It is worth pointing out here, as is indeed well-known by now, that to solve the VCC scattering equations within the rotationally sudden scheme implies that the simultaneous energy transfer by collision to the molecular rotational and vibrational degrees of freedom is treated on a different footing, at least from the dynamical viewpoint. In other words, what one is saying here is that the perturbation induced by the weak interaction on the vibrational excitation requires, especially at low relative collision energy, the dynamical coupling of the diabatic states of the target via the off-diagonal matrix elements of eq 10 in order to yield a realistic estimate of the small inelastic cross sections. On the other hand, the rotationally inelastic processes (which have been shown earlier by us[8] to be caused by the short-range part of a highly anisotropic interaction) can be considered to occur on a different time scale so that those excitation processes can be decoupled from the vibrationally inelastic collisions and introduced, *after* the vibrational dynamics, via the weighted convolution of eq 16 over different atom−molecule orientations at which the vibrational CC problem has been solved. Such an assumption is obviously dependent on various factors and, all things being equal, on the relative collision energies for which the inelastic process is evaluated. We shall show below that such an assumption breaks down close to the opening of the vibrational thresholds.

A more rigorous way of describing the quantum dynamics of the rotovibrational excitation process is therefore obtained by including *both* rotational and vibrational coupling between relative motion and internal degrees of freedom during the collision dynamics. This corresponds to solving the full CC rotovibrational equations for the collisionally inelastic cross sections, either state-to-state or partially summed over states.[19] One therefore requires the calculations of the relevant **T**-matrix elements, $T^J_{v'j'l',vjl}(E)$, by solving more extended coupled equations which explicitly include the coupling, during the scattering process, of rotational and vibrational channels via the perturbing potential.[20] From the knowledge of the individual matrix elements one then obtains the corresponding partial quantities:

$$A^J{}_{vj\to v'j'}(E) = c_j\sum_{l,l'}|T^J_{v'j'l',vjl}|^2 \quad (19)$$

with

$$c_j = \frac{4\pi}{k_j^2(2j+1)} \quad (20)$$

where $|vj\rangle$ and $|v'j'\rangle$ correspond to the quantum numbers of the initial and final molecular states. The partial amplitudes $A_l(vjm \to v'j'm')$ which appear in the expression for the state-to-state differential cross sections[20] are related to additional averaged quantities which can be ultimately extracted from eq 19.

$$A^{l'}_{vj\to v'j'}(E) = c_j\sum_{mm'}|A_l(vjm \to v'j'm')|^2 = c_j\sum_{Jl}|T^J_{v'j'l',vjl}|^2 \quad (21)$$

Hence one can write[20]

$$\sum_J A^J_{vj\to v'j'}(2J+1) = \sum_{l'}(2l+1)|A^{l'}_{vj\to v'j'} \quad (22)$$

The corresponding state-to-state integral cross sections that we are seeking to calculate here are given by

$$\sigma_{vj\rightarrow v'j'}(E) = \sum_J \sigma^J_{vj\rightarrow v'j'} = \sum_J (2J+1)A^J_{vj\rightarrow v'j'} = \sum_{l'} \sigma^{J'}_{vj\rightarrow v'j'} = \sum_{l'} (2l+1)A^{l'}_{vj\rightarrow v'j'} \quad (23)$$

from which one can also define the partial wave contributions to the CC cross sections as given by[20]

$$\sigma^{J(l)}_{vj\rightarrow v'j'} = P^{J(l)}_{vj,v'j'} \quad (24)$$

As is well-known, the transition matrix elements are in turn related to the scattering **S**-matrix elements, the absolute square of which gives us the transition probabilities for each inelastic, state-to-state process.

$$S^J_{vjl\rightarrow v'j'l'} = \delta_{jj'}\delta_{ll'}\delta_{vv'} - 2iT^J_{vjl,v'j'l'} \quad (25)$$

Because of the rapid increase in the number of target rotational states that become energetically open as the collision energy increases, and because of the multiplicity effects in eq 19, the number of coupled equations in the rotovibrational problem becomes rapidly very large and therefore computationally very costly. On the other hand, the study of purely rotational excitation processes in the present system[8] has already shown that the present interaction, although rather strongly orientation dependent, is also a short-range interaction where a rather limited number of trajectories, or partial waves, is involved at low collision energies. Thus, it becomes both reasonable and expedient to introduce a more approximate treatment of the angular momentum recoupling during the quantum dynamics which goes under the name of coupled state (CS), or centrifugal sudden, approximation.[21−23] The vibrational degree of freedom, on the other hand, is still treated with the correct CC scheme.

One therefore removes the coupling degeneracy given by each pair of (l,l') angular momenta of the entrance and exit channels by considering only one value of $\bar{l}$ as contributing to the double sum from eqs 21 and 23. Physically, this means that the collision process is seen as being dominated by short-range forces, and therefore it is reasonable to assume that no change of the initial l into a final l' value is occurring in the dynamical recoupling during the scattering process when the rotational energy (angular momentum) content of the target is varied. In other words, one keeps the correct vibrational coupling by the potential and correctly includes the further coupling of vibrational levels with the rotational levels due to the anisotropic torque applied by the scattering event, but simplifies the number of coupled equations by disregarding the rotor reorientation after the scattering (j_z conserving approximation[20,23]).

Thus far we have employed the quantum treatment to generate state-to-state partial cross sections on the energy shell. By further averaging their energy dependence over a Boltzman type velocity distribution, one can then obtain the corresponding state-to-state excitation or relaxation rates:

$$k_{jv\rightarrow j'v'}(T) = 4\pi\left(\frac{\mu}{2\pi k_B T}\right)^{3/2} \int_0^\infty \sigma_{jv\rightarrow j'v'}(v) \exp\left(\frac{\mu v^2}{2k_B T}\right) v^3 \, dv \quad (26)$$

where k_B is the Boltzman constant and v is the relative velocity between colliding partners.

Further quantities that can give us some indication on the system efficiency in collisionally populating higher levels of the LiH target are the average rotovibrational (state-to-state) energy transfer index as a function of collision energy E:

$$\Delta E_{\text{rotvib}}(E,v,j) = \left(\sum_{j',v'} \sigma_{jv\rightarrow j'v'}(E)\Delta\epsilon_{jv,j'v'}\right)\left(\sum_{j',v'} \sigma_{jv\rightarrow j'v'}\right)^{-1} \quad (27)$$

where $\Delta\epsilon_{jv,j'v'}$ is the energy spacing between two rotovibrational levels $|jv\rangle$ and $|j'v'\rangle$. A more averaged quantity that gives the rotationally summed vibrational energy transfer for the process considered is instead

$$\Delta E_{\text{vib}}(E,v) = \left(\sum_{v'}\sum_{j,j'} \frac{1}{(2j+1)} \sigma_{jv\rightarrow j'v'}\Delta\epsilon_{jv,j'v'}\right) \times \left(\sum_{v'}\sum_{j,j'} \frac{1}{2j+1} \sigma_{jv\rightarrow j'v'}\right)^{-1} \quad (28)$$

If one considers the more likely populational situation in the interstellar medium and in the protogalactic clouds, then only the $v = 0$ target states need to be considered. Thus, the vibrational energy transfer of eq 27 that interests us most is the one from $v = 0$ that becomes the energy transferred into excited vibrational and rotational levels for different initial rotational levels within the $v = 0$ manifold, the $\Delta E_{\text{vib}}(E,o,j)$. By the same token, the quantity defined by the further averaging and summing carried out by eq 28 could be taken, when from the $v = 0$ only, to be the $\Delta E_{\text{vib}}(E)$.

In evaluating the efficiency of the collisional energy transfer processes it is also useful to take into consideration temperature effects within the medium, i.e., to try to estimate what type of thermal averaging would be more useful to consider. In the case of the excitation of LiH molecules which are in their $v = 0$ vibrational level, one could consider at first a distribution function for the relative collisional energies in the medium when the collision frequencies become high enough to induce translation thermalization. Thus, the simplest form of the distribution function is the Boltzmann distribution for any given number density value of the species, n, in units of molecules × cm^{-3}.

$$f(E,T) = \frac{2}{\sqrt{\pi}}\frac{n}{(k_B T)^{3/2}} \sqrt{E} \exp(-E/k_B T) \quad (29)$$

which allows us to evaluate the following quantity:

$$dE_{\text{vib}}(T,j) = \int_0^\infty \Delta E_{\text{vib}}(E,j)\, f(E,T)\, dE \quad (30)$$

which considers the molecules to be in a given rotational state of the $|o,j\rangle$ manifold. The further averaging over the rotational population at the same macroscopic T value as that reached by the translational thermalization yields now

$$\langle \Delta E_{\text{vib}}\rangle_{\text{tot}}(T) = \sum_j g_j(T)\, \Delta E_{\text{vib}}(T,j) = \sum_j \Delta E_{\text{vib}}(T,j) \exp(-\epsilon_j/k_B T) \quad (31)$$

Another quantity of interest is the collisional heating function, CHF, defined as the ratio between a chosen inelastic flux into

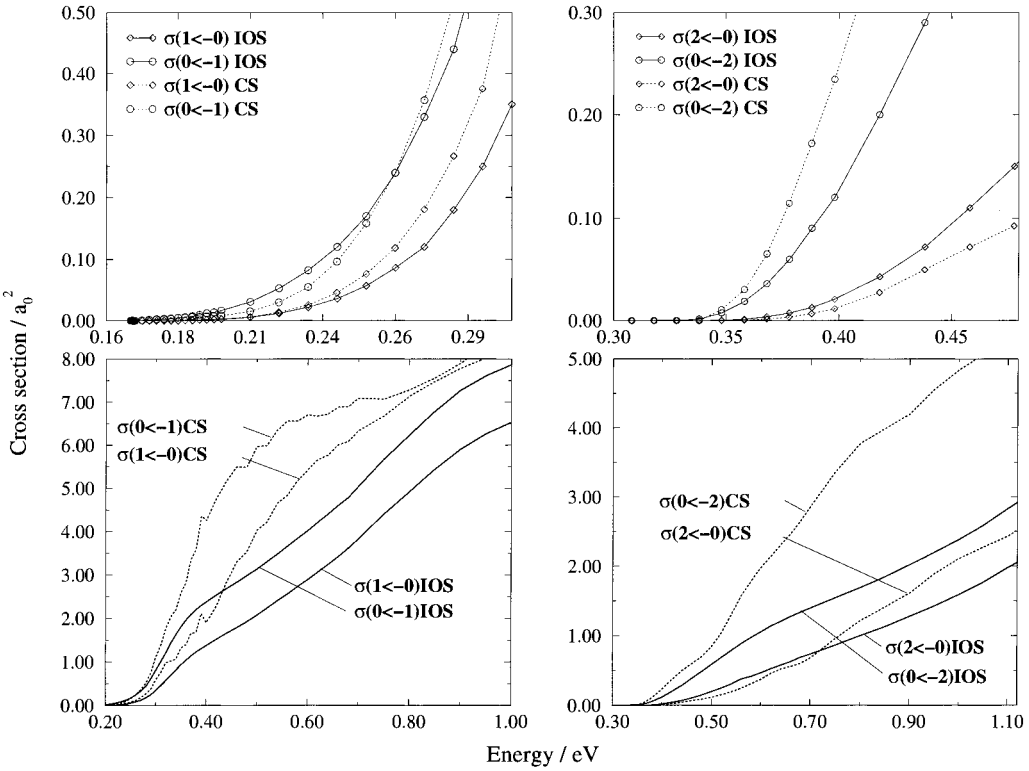

Figure 2. Computed, rotationally summed vibrationally inelastic cross sections for the excitation and relaxation processes involving the (0, 1) levels, left, and the (0, 2) levels, right. The calculations employ the VCC-RIOS coupling scheme (dashed curves) and the VCC-RCS coupling scheme (solid curves). Two different ranges of energy are shown for both sets of collisional transitions.

excited channels and the overall collisional flux:

$$\mathrm{CHF}(E,j) = \frac{\sum_{v\neq 0}\sum_{j'\neq j}\sigma(0j \rightarrow v,j'|E)}{\sum_{v,j'}\sigma(0j \rightarrow vj'|E)} \tag{32}$$

$$\mathrm{CHF}(T,j) = \int_0^\infty \mathrm{CHF}(E,j)\, f(E,T)\, \mathrm{d}E \tag{33}$$

$$\langle \mathrm{CHF}(T)\rangle_{\mathrm{tot}} = \sum_j \mathrm{CHF}(T,j)\, g_j(T) \tag{34}$$

The above quantities give us some indication of the overall efficiency of the excitation process, starting from the $v = 0$ state, with respect to the elastic collisions which do not manage to form internally "hot" target molecules. We shall see below that the evaluation of average energy transfer indices and collisional heating functions can help us to understand better the microscopic behavior of the single-collision events.

4. The Computed Collisional Quantities

As mentioned earlier, the basic quantities needed to model the collisional heating of LiH interacting with He atoms in a single-collision situation are the individual, partial integral cross sections involving rotational and vibrational states of the target molecule. We have therefore computed such quantities using both the VCC-RIOS coupling scheme described in the previous section and its more accurate recoupling approximation, which we have called the VCC-RCS dynamical treatment.

Given the range of action of the vibrational coupling, the target-bound vibrational states up to $v = 4$ were taken into the expansion since the corresponding wave functions were those included within the range of r values actually computed to obtain the full PES.[8,13] The integration on the radial variable was extended up to $R_{\max} = 30.0\ a_0$, while the range of angular momenta went up to $l_{\max} = 240\hbar$. The angular integration within the VCC-RIOS treatment included 27 different angular values reached by interpolation between the computed orientations discussed before.[8] Within the CS treatment of rotational coupling the rotational states were included up to $j_{\max} = 16$ for $v = 0,1$ and up to $j_{\max} = 14$ for $v = 2$. For the $v = 3$ channel $j_{\max}$ was taken up to 7. The numerical convergence of the **S**-matrix elements required the inclusion of at least two closed vibrational states. Finally, the integration over the energy range to yield all the temperature-dependent quantities involved at least 100 different energy values.

The diagrams shown in Figure 2 report the behavior of the computed vibrationally (rotationally summed) inelastic cross sections (VCC-RIOS and VCC-RCS) for both the excitation and relaxation processes in the lower range of collision energies (upper diagrams) and for the higher set of collision energy (lower diagrams). The diagrams on the left in the figure (top and bottom) correspond to the $\Delta v = 1$ processes, while the diagrams on the right (top and bottom) correspond to the $\Delta v = 2$ processes. It is interesting to note the following:

(i) As the collision energy moves away from threshold, the CS cross sections become consistently larger than the IOS cross sections, indicating that the correct recoupling of angular momenta via this strongly anisotropic potential has a marked effect on vibrational inelasticity, as we shall further discuss below.

(ii) The $(0 \rightarrow 2)$ excitation cross sections, although smaller than the single-transition cross sections, are still within the same order of magnitude, further indicating the cooperative effect of efficient rotovibrational processes in favoring vibrational excitation mechanisms.

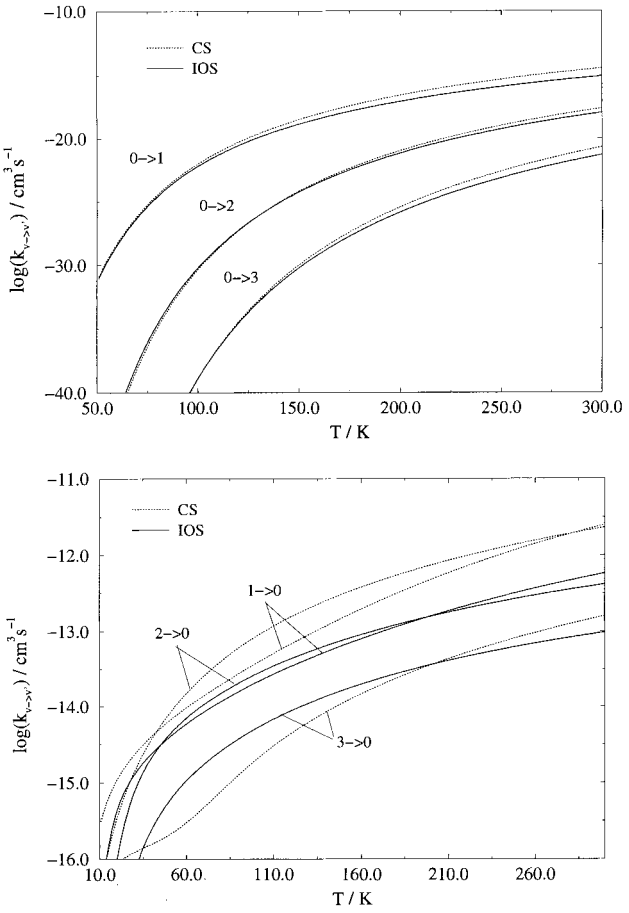

Figure 3. Computed excitations and relaxation rates, for temperatures up to 300 K, for the transitions with $\Delta\nu = 1$, 2, and 3. The VCC-RIOS results are given by the solid lines, while the VCC-RCS results are given by the dashed lines.

(iii) At energies just above thresholds, the CS cross sections exhibit more structure than their IOS counterpart and indicate the presence of low-energy resonances due to the effective potential provided within the CS scheme: their specific features will be discussed elsewhere.[13]

(iv) Removal of the energy sudden approximation for the rotational levels when going from the IOS to the CS calculation of cross sections causes larger differences in the cross sections themselves when the collision energy is increased since more states become energetically open and are dynamically coupled by the anisotropy of the PES.

As a preliminary conclusion, one may say that the roto-vibrationally inelastic collisions in the present system are reflecting the broad features of the PES involved: strong anisotropic features and rather weak vibrational coupling which however gets strongly tied to the rotationally inelastic energy transfers occurring within the vibrational manifolds.

The results of Figure 3 report the corresponding rates for vibrationally inelastic processes over the range of temperatures from threshold to about 300 K. The upper part of the figure shows the excitation processes from the ground vibrational state of the target (and rotationally summed) into the lower excited vibrational states up to $v' = 3$. The lower diagram, on the other hand, reports the relaxation collisional rates into the ground vibrational level of LiH.

It is remarkable to note that the excitation rates even in the lower T range are showing the CS results to be invariably larger than their IOS counterparts. At higher temperatures even larger differences exist between IOS and CS results up to temperatures beyond about 300 K. This result suggests that, already from collision energies close to the threshold values, the rotational excitation mechanism must be taken to be strongly coupled to the vibrational excitation mechanism. As the collision energy increases, the presence of a greater number of rotational target states which are energetically open, and correctly treated in the CS scheme, does make a difference and markedly affects the values of cross sections and rates at higher temperatures.[13]

It is also surprising to note the actual size of the excitation/relaxation rates of Figure 3: in spite of the weak nature of the present interaction, in fact, one finds that the vibrationally inelastic process is much more probable than in the case of CO[24] or of HF[25] interacting with the same rare gas. The strong orientational dependence of the present system, therefore, does play an important role in driving flux into the inelastic channels, both rotational[9] and vibrational. The behavior of the efficiency indices described in the previous section is shown by the results presented in Figures 4 and 5.

It is interesting to note from the results on the average energy transfer index (in units of meV), shown as a function of collision energy on the left of Figure 4, that the CS calculations suggest fairly large values of such quantities but only after a very slow start at low collision energies. When looking at the individual cross sections, one sees that the rotationally inelastic processes are in fact contributing in a marked way to the energy transfers since we see that the ΔE_{vib} values from the larger j of the manifold are smaller than those from the lower j, especially at higher collision energies.

The corresponding temperature dependence assumes, to take on a simple model, a thermal distribution for the relative collision energies and convolutes numerically the average energy transfer indices of before. We see that such quantities, presented for a unit number density value (one molecule/cm^3), vary greatly over the range of T considered and show that they rapidly span nearly 20 orders of magnitude over a range of 3000 K. The same is true when thermal averaging of the rotational population is included, where the $\langle \Delta E_{vib} \rangle_{rot}$ values become also several orders of magnitude larger at the higher T.

The additional indices defined before by eqs 32−34 are reported in Figure 5 as a function of energy and for several initial j states (on the left) and as a function of temperature (on the right). The further rotational averaging once again makes the total CHF factors larger at higher temperatures. Furthermore, the slow onset of these factors at low energies, and their change by several orders of magnitude over the examined range of temperatures, underlines the crucial role played by the rotational energy ladders in funneling energy into the vibrationally excited molecules.

5. Summary and Conclusions

In the present work we have discussed, after producing for the first time quantitative estimates of it, the collisional efficiency of exciting LiH molecules to their $v = 1$, 2 vibrational levels and to corresponding manifolds of open rotational levels by collisions with He atoms.

The processes have been treated as quantum collisional events, and we have employed an ab initio potential energy surface that correctly couples the anisotropy of the interaction with the range of action of the vibrational perturbation by the impinging He atom. The dynamical effects caused by the rotational states of the target, which are coupled with the collisional (translational) angular momentum via the computed PES, were considered within different coupling schemes, and

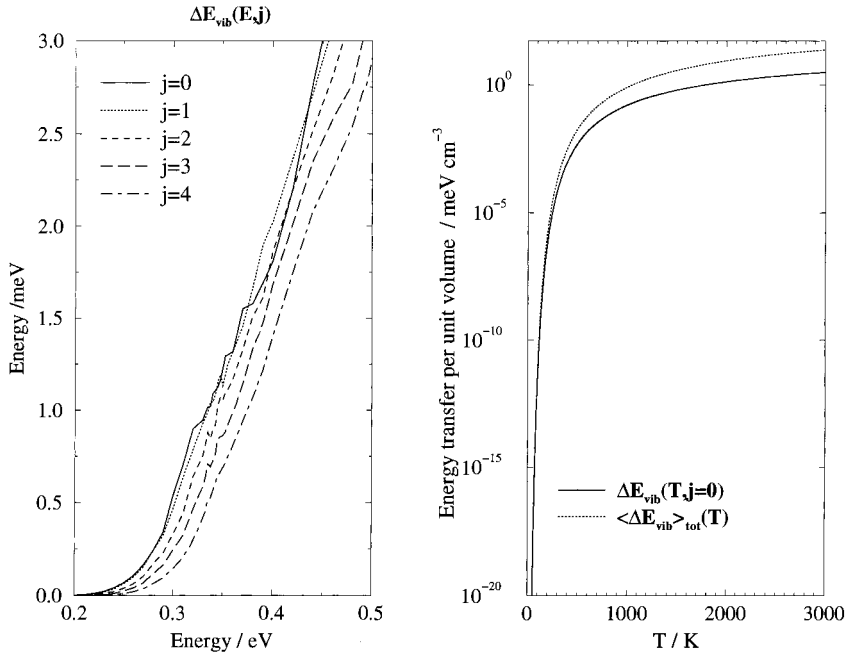

Figure 4. Computed average energy transfer values (in meV) for different initial rotational levels of the target and from the $v = 0$ initial vibrational state of LiH. Left: results as a function of energy. Right: results as a function of temperature (solid line, averaging from the $j = 0$ level; dashed line, further averaging over rotational levels). Values for a number density of one molecule $\times$ cm^{-3}.

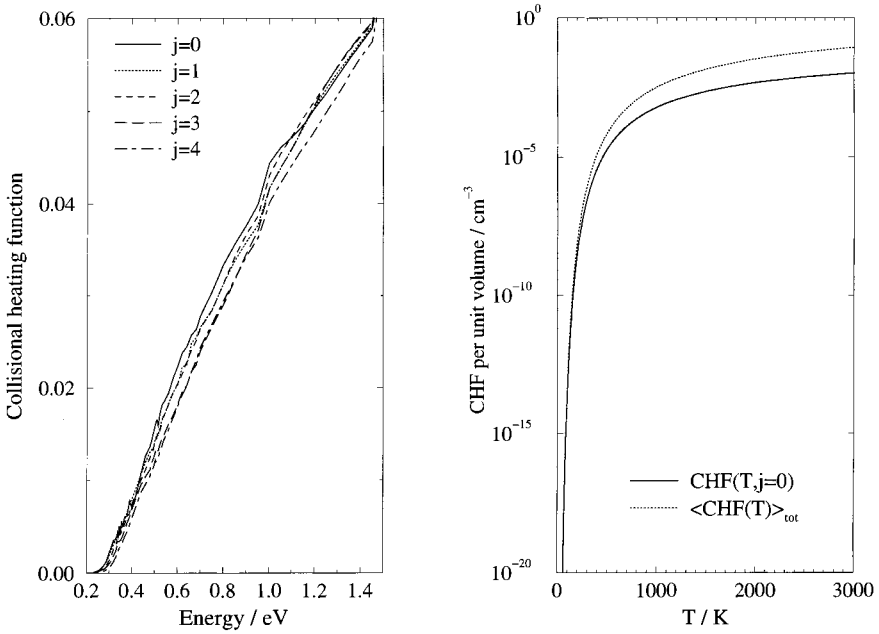

Figure 5. Computed collisional heating functions, CHF, following eqs 32−34 of the main text. The values are labeled like the quantities of Figure 4: as a function of energy (left) and as a function of temperature (right).

the results for both the final inelastic cross sections and the excitation rates were compared with each other.

We had already found in our earlier study[9] that the strong orientational anisotropy of the present system causes the rotational inelastic component of the collisional energy transfer to be particularly large in spite of the weak nature of the vdW interaction. We further find here that the vibrational coupling is not very strong and rather short-ranged in character, as we have also extensively discussed elsewhere.[13] Thus, the roto-vibrationally inelastic cross sections come out to be fairly large mostly because of the cooperative effects from the rotational energy ladders where rather large Δ_j transitions are still seen to have a non-negligible probability[9] (cross sections). The corresponding rotovibrational excitation rates are therefore found markedly larger than those exhibited by, say, the He−CO system[24,26] over the same range of temperatures. Furthermore, the present results allow us to obtain a more quantitative estimate of the energy and temperature behavior of some collisional efficiency indicators, which can in turn help us to formulate more realistic imput parameters for a global modeling of primordial clouds.[1,3] The previous discussion has shown that the average energy transfer index starts out very small at low T and so does the collisional heating function CHF (both presented in Figures 4 and 5), while they grow to very large values up to $T \approx 3000$ K. This means that the possibility exists for forming rotovibrationally "hot" LiH molecules not only by radiative recombination[2] but also by collisional excitations with other, abundant species in the protogalactic clouds such as the He

atoms.[4] In conclusion, the present calculations, which carried out a quantum description of the energy transfer dynamics to LiH, allow us to show for the first time a realistic estimate of collisional excitation probabilities for such molecules and therefore provide a further piece of information to realistically produce a fuller modeling of the kinetics of molecular formation in the early universe. The extension of this study to H and H^+ projectiles is currently under way in our laboratory and will be reported in the near future.

Acknowledgment. The financial support of the Italian National Research Council (CNR) and of the Italian Ministery for University and Research (MURST) is gratefully acknowledged. One of us (S.K.) also wishes to thank the Max-Planck-Society for the financial support of his stay in Rome, during 1997, through the M.P. Research Prize awarded to F.A.G.

References and Notes

(1) Lepp, S.; Shull, J. *Astrophys. J.* **1984**, *425*, 372.
(2) Gianturco, F. A.; Gori Giorgi, P. *Astrophys. J.* **1996**, *479*, 560, and references quoted therein.
(3) Palla, F.; Salpeter, E. E.; Stahler, S. W. *Astrophys. J.* **1983**, *271*, 632.
(4) Wagoner, R.; Fowler, W. A.; Hoyle, F. *Astrophys. J.* **1967**, *148*, 3.
(5) Dubrovich, V. K. *Astron. Lett.* **1993**, *19*, 53.
(6) De Bernardis, P.; Dubrovich, V.; Encrenaz, P.; Maoli, R.; Masi, S.; Mastrantonini, G.; Melchiorri, B.; Melchiorri, F.; Signore, M.; Tanzilli, P. E. *Astron. Astrophys.* **1993**, *269*, 1.
(7) Peebles, P. J. E. *Principles of Physical Cosmology*; Princeton: Princeton University Press, 1994.
(8) Gianturco, F. A.; Kumar, S.; Pathak, S. K.; Raimondi, M.; Sironi, M. *Chem. Phys.* **1997**, *215*, 239.
(9) Gianturco, F. A.; Kumar, S.; Pathak, S. K.; Raimondi, M.; Sironi, M.; Gerrat, J.; Cooper, D. L. *Chem. Phys.* **1997**, *215*, 227.
(10) Cooper, D. L.; Gerratt, J.; Raimondi, M. *Adv. Chem. Phys.* **1987**, *69*, 319.
(11) Matias, M. A.; Raimondi, M.; Tornaghi, E.; Cooper, D. L.; Gerratt, J. *Mol. Phys.* **1994**, *83*, 89.
(12) Silver, D. M. *J. Chem. Phys.* **1980**, *72*, 6445.
(13) Bodo, E.; Kumar, S.; Gianturco, F. A.; Sironi, M.; Raimondi, M. *Chem. Phys.*, in press.
(14) Schinke, R. *Chem. Phys.* **1977**, *24*, 379.
(15) Parker, G. A.; Pack, R. T. *J. Chem. Phys.* **1978**, *68*, 1585.
(16) Gianturco, F. A.; Kumar, S. *J. Chem. Phys.* **1995**, *103*, 2940.
(17) Gianturco, F. A.; Kumar, S. *J. Chem. Phys.* **1995**, *99*, 15342.
(18) Gianturco, F. A.; Kumar, S. *J. Chem. Phys.* **1995**, *196*, 485.
(19) Gianturco, F. A.; Serna, S.; Palma, A.; Billing, G. D.; Zenevich, V. *J. Phys. B, At. Mol. Opt. Phys.* **1993**, *26*, 1839.
(20) For a detailed presentation see: Gianturco, F. A. *The Transfer of Molecular Energy by Collisions*; Springer Verlag: Berlin, 1997.
(21) McGuire, P. *Chem. Phys.* **1974**, *4*, 483.
(22) McGuire, P.; Kouri, D. J. *Chem. Phys.* **1974**, *60*, 2488.
(23) Shimoni, Y.; Kouri, D. J. *J. Chem. Phys.* **1977**, *66*, 2841.
(24) Gianturco, F. A.; Paesani, F.; Buonomo, E. In preparation.
(25) Gianturco, F. A.; Bernardi, M. *J. Chem. Phys.* **1989**, *93*, 7629.
(26) Reid, J. P.; Simpson, C. J. S. M.; Quiney, H. H.; Hutson, J. M. *J. Chem. Phys.* **1995**, *103*, 2528.